applied sciences

MDPI

*Article*

# Resonant Acoustic Metamaterials

**Gino Iannace [1,*], Giovanni Amadasi [2], Antonella Bevilacqua [3], Maria Cairoli [4] and Amelia Trematerra [1]**

[1] Department of Architecture and Industrial Design, University of Campania "Luigi Vanvitelli", 81031 Aversa, Italy; liatrematerra@libero.it
[2] SCS-ControlSys—Vibro-Acoustic, 35011 Padova, Italy; g.m.amadasi@scs-controlsys.com
[3] Department of Architecture and Engineering, University of Parma, 43124 Parma, Italy; antonella.bevilacqua@unipr.it
[4] Energy Department, Politecnico di Milano, 20133 Milano, Italy; maria.cairoli@polimi.it
* Correspondence: gino.iannace@unicampania.it

**Abstract:** Acoustic applications of metamaterials have rapidly developed over the past few decades. The sound attenuation provided by metamaterials is due to the interaction between soundwaves and scatterers organized into a reticular grid, with a peak attenuation at a specific frequency band that is highly dependent on the scatterers' diameter and reticular geometric organization of installation. In this article, the scatterer types chosen for the experiments are represented by a 2D shape, which are cylindrical solid-wood bars of 15 mm diameter and empty cylindrical bars of 20 mm diameter. Acoustic measurements were conducted in a semi-anechoic chamber to identify the specific frequency at which the highest insertion loss (IL) was registered. A second experiment was conducted by creating holes of 5 mm diameter on the external surface of the empty bars; in this way, it registered a higher sound attenuation. In particular, the resonant system characterized with holes, in combination with the attenuation given by 2D scatterer metamaterials, increased the sound attenuation for the frequency range between 1 kHz and 10 kHz.

**Keywords:** metamaterials; insertion loss; scale model; noise attenuation; diffraction; 2D scatterers

**Citation:** Iannace, G.; Amadasi, G.; Bevilacqua, A.; Cairoli, M.; Trematerra, A. Resonant Acoustic Metamaterials. *Appl. Sci.* **2024**, *14*, 5080. https://doi.org/10.3390/app14125080

Academic Editor: Douglas O'Shaughnessy

Received: 9 May 2024
Revised: 2 June 2024
Accepted: 8 June 2024
Published: 11 June 2024



## 1. Introduction

The theory of metamaterials was developed in the 1960s with the goal of changing the direction of propagation of the electro-magnetic waves and creating an element (or a system of different elements) with negative refraction [1]; this material should not create resistance to the propagation of soundwaves or allow the wave to pass through without generating any reflection [2]. It should be remembered that negative refraction is the electromagnetic phenomenon where light rays become refracted at an interface that is opposite to their more commonly observed positive refractive properties. Research in the field of electro-magnetic waves brought the application of metamaterials to telecommunications, optics, and other areas.

The term metamaterial was obtained by combining the Greek word "meta", meaning beyond, with the Latin word "materia", meaning material, whereby a metamaterial is a material designed to have physical properties that are not found in nature [3].

Research on metamaterials can develop if supported by complex geometry realized with a 3D printer. A great role in this direction is played by the volumes and geometry variation following a periodic configuration, obtaining more precise control of sound attenuation in a desirable frequency range. One of the applications in acoustics is represented by sonic crystals with the aim of reducing acoustic pollution by taking advantage of destructive interferences [4].

Research on the creation of barriers to limit the noise generated by road traffic has been carried out by many authors who have highlighted the importance of having noise attenuation by using innovative systems. Metamaterial acoustic barriers have been

proposed to reduce train noise, especially the noise emitted by the friction between wheels and rails, with the installation of mini barriers composed of a height equal to the train wheels [5].

Some authors have proposed 3D structures of metamaterials made with spheres of different diameters (i.e., 20 mm, 30 mm and 40 mm). Holes made on the external surface of the hollow spheres create a resonant effect and increase the sound attenuation [6].

Another field where regular structures can be applied is related to the acoustic absorption of membrane systems. A membrane placed at a certain distance from a rigid surface optimizes the sound absorption at a frequency equal to $\lambda/4$. In other words, if the cavity thickness between the membrane and solid back surface is 0.8 m, this system is tuned to absorb a sound at 100 Hz [7]. It shall also be said that the sound absorption varies in function depending on the masses applied to the membrane, which are capable of widening the range of absorption and/or moving the peak onto other frequency bands [8].

Research on the application of metamaterials has been extended to the control of building structures during earthquakes up to heating transmission and acoustics with the theory of sound crystals [3]. Regarding this latest concept, the sound attenuation created on a destructive interference occurs at a frequency whose wavelength is comparable to the dimension of scatterers and to the distance existing among each other. It has been reported that the higher the distance between scatterers, the lower the frequency at which the maximum sound attenuation occurs. Therefore, by controlling the distance between scatterers, it is possible to achieve the maximum sound attenuation at the desirable octave, a phenomenon that cannot be executed with the traditional absorbing panels.

### *1.1. Metamaterials across History: The Beginning*

A historical concept of the realization of metamaterials can be represented by the glass cup of Lycurgus in ancient Rome, dated back to the 4th century and preserved in the British Museum. This cup shows different ray color diffraction based on the direction of the light passing through the glass, which is green when the cup is highlighted from the front, and red when the cup is highlighted from behind. This effect is obtained by the insertion of little fragments of gold and silver in a colloidal organization on the external surface of the glass [9].

Similarly, the glass composition of the Gothic churches of northern Europe in the Middle Age were realized with metamaterial structures.

### *1.2. Employment of Metamaterials in the Last Century*

In modern times, a different application of metamaterial occurred during World War II [10], when the German submarines were coated with rubber [11] elements equipped with holes on a regular grid to recreate the Helmholtz resonator system to prevent being detected by the English navy [12]. This approach was named Alberich, following the legend of a warrior fighting with an invisible mantel. Nowadays, submarines have similar structures to be invisible to sonars [13]. In underwater acoustics, this type of highly absorbing coating is employed to cover the surface of offshore structures to control the negative effects on marine mammals due to high levels of noise during propagation [14,15].

In the last century, research studies by V. Veselago were focused on the discovery of a specific material with negative refraction that, after being hit by an electro-magnetic wave [16], should not create resistance to the propagation and allow the wave to pass through without generating any type of reflections, with a potential goal of achieving a negative refraction index [17]. These studies were thereafter deepened by J. Pendry for the design of lenses by utilizing negative metamaterials to achieve the focus of light to improve eyesight [1,18].

Many artists in history were considered leaders in creating masterpieces based on the effects on the interaction between waves and solid surfaces [19]. An example is the organ structure by Eusebio Sempere, whose sculpture is located in the garden belonging to the Juan March Foundation in Madrid, Spain [20]. Sempere applied a minimalist design

composed of a very simple geometry of steel bars of 30 mm diameter, organized in a 2D grid with a 100 mm distance between each other. This sculpture represents the first example of a bidimensional periodic sculpture. The acoustic measurements conducted on this sculpture highlight a certain attenuation in the range between 1.6 kHz and 5 kHz [21].

## 2. Acoustic Characteristics of Metamaterials

Metamaterial structures can be classified into the following three sectors based on the geometry of scatterers, as shown in Figure 1:

- The scatterers are planes, and their structure is periodic in only one direction is the case of 1D scatterers.
- The scatterers are cylindrical, and their structure is periodic in two orthogonal directions is the case of 2D scatterers.
- The spherical scatterers characterize the third type of metamaterials with their three periodic directions.

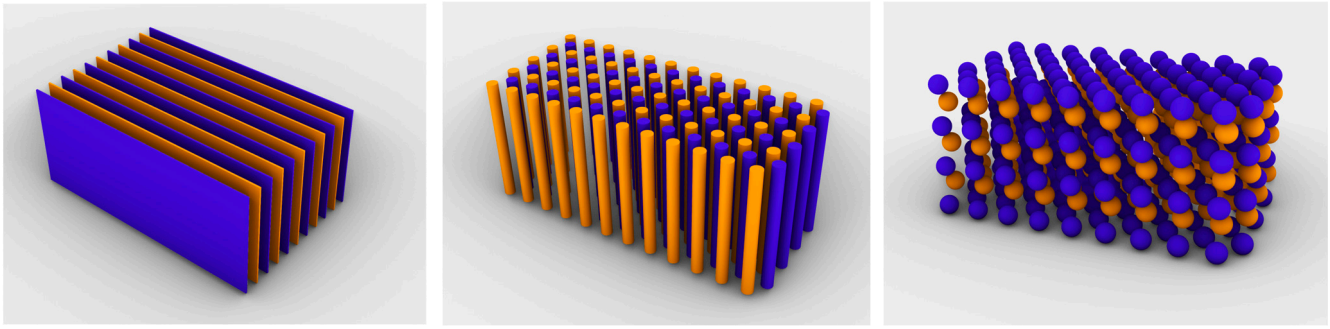

(**a**) (**b**) (**c**)

**Figure 1.** Disposition of scatterers in the 1D periodic direction (**a**), 2D periodic directions (**b**), and 3D periodic directions (**c**).

Metamaterials are artificial structures used to obtain sound attenuation. Based on this concept, research focused on noise control is increasing.

The soundwave propagation control provided by the structures of metamaterials is obtained by the interaction between the regular disposition of their geometric scatterers and the effect of incident waves passing through them [22]. This phenomenon is achievable with the principle of a destructive interference between waves during the propagation through the scatterers and is described by Bragg's law that was initially applied to the electro-magnetic field. In acoustics, the attenuation frequency $f_{BG}$ is calculated as per Equation (1).

$$f_{BG} = \frac{c}{2\alpha \sin(\phi)} \quad (1)$$

where $c$ is the sound speed in the air (344 m/s), $a$ is the distance between scatterer structures and $\phi$ is the incident angle.

The propagation scheme of sound waves hitting a regular geometric grid is shown in Figure 2. The scatterers are organized with a constant step along the horizontal line.

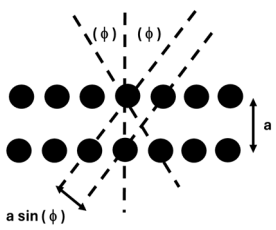

**Figure 2.** Soundwave propagation scheme when an incident wave impacts against a regular geometric structure.

When the scatterers' dimensions are comparable to the wavelength of the incident wave, a destructive interference occurs and, consequently, an attenuation of the soundwave energy passing through the metamaterial structure is achieved. In addition, it should be said that the attenuation is not particularly dependent on the material applied to the scatterers, but more on the geometry of the single elements [23].

A research application of 2D scatterers has been developed for the attenuation of noise related to domestic noise, with the creation of a "meta-house" composed of cylinders organized at a constant step onto a regular grid [24]. The experiments on this type of structure were conducted on a scaled model of 1:10, with a maximum attenuation equal to 18 dB recorded between 1.5 kHz and 15 kHz, as shown in Figure 3. If applied to transparent material-like polymers, this solution can satisfy conditions of acoustic comfort [25], lighting and ventilation requirements [26]. In general, the acoustic performance of metamaterial structures and sonic crystals can be measured with the insertion loss (*IL*) expressed in decibels (dB) [27] that is given by the level difference calculated with and without the installation of the structure between the source and receiver, as indicated in Equation (2).

$$IL = L_{withou} - L_{with}\ (\mathrm{dB}) \quad (2)$$

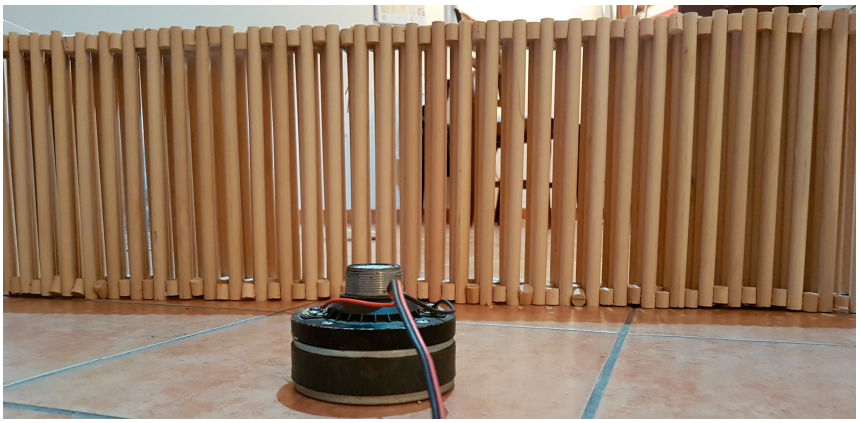

**Figure 3.** Scale model of metamaterial acoustic barrier.

## 3. Research Methodology: Resonant System Configurations and Test Conditions

The scope of this paper is the study of a different type of scatterers used to improve acoustic absorption, including 2D scatterers and 2D scatterer resonators [28,29]. Two-dimensional scatterer resonators refer to a system composed of empty cylinders equipped with a series of holes on the external surface (resonators) that connect the cavity to the exterior, which are constantly re-distributed [30]. Applications of this type of resonant scatterers can be represented by the creation of acoustic filters for the noise attenuation of fans in cooling systems and for the attenuation of road traffic noise [31].

In this paper, acoustic measurements were conducted inside a semi-anechoic chamber of 4.4 × 4.4 × 4.5 m, characterized with absorption on the walls and ceiling, and concrete-finish flooring. Figure 4 shows the equipment employed during the acoustic measurements, with the set-up scheme created for the performance of *IL* measurements [32]. The loudspeaker was fed a pink noise equalized over all the frequency bandwidth [33] and placed in a box whose surfaces were coated with absorbing mats to stop any potential standing waves. This box has an openable lid at the top, where the metamaterial acoustic element was installed. An omnidirectional microphone was installed at 1 m from the test sample. The acoustic tests were carried out with the following two specific configurations to calculate the *IL*:

- Sound-pressure-level difference measured without samples.
- Sound-pressure-level difference measured with the test samples.

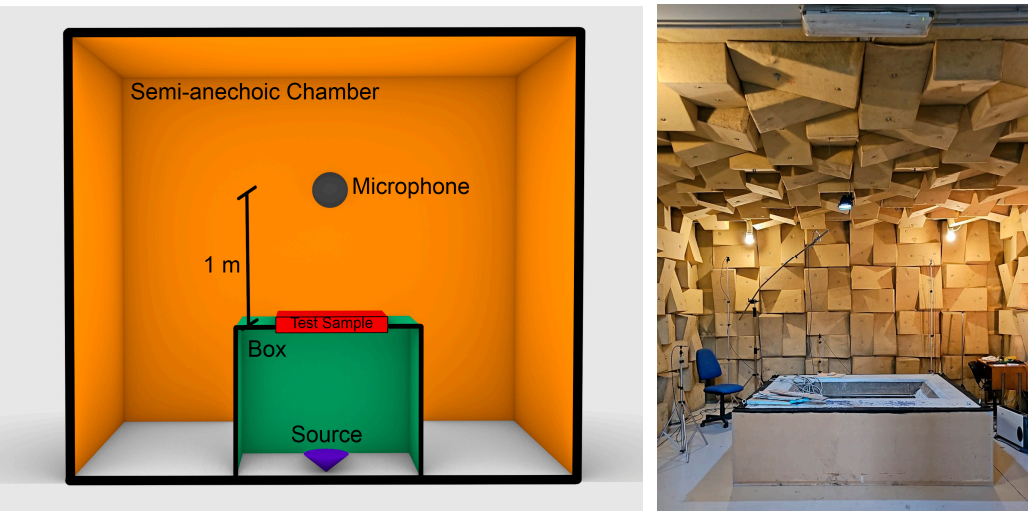


**Figure 4.** Equipment scheme during the acoustic measurements (**left**). View of the laboratory during the measuring tests (**right**).

A smaller box was built to better assess the *IL* attenuation of the noise that was generated by the loudspeaker and passed through the test sample. The dimensions of the box were 1.2 × 1.3 × 0.5 m.

The implementation of this measurement scheme allowed the computation of the attenuation to only involve the function of the interference given by the scatterers [34], excluding the diffraction effects of the edges.

The acoustic measurements were out on the following test samples:

- Smooth wooden scatterers of 15 mm diameter with the addition of a plastic empty scatterer of 20 mm diameter with a 1.5 mm thickness.
- Five holes of 5 mm diameter were created on the external surface of the plastic empty scatterers. The length of the bar is always kept constant, equal to 300 mm for all tests, as shown in Figure 5.

The samples were tested individually based on the following configurations:

- Configuration A1, composed of 1 row of wooden scatterers with a 15 mm diameter.
- Configuration A2, composed of 2 rows of wooden scatterers of 15 mm diameter, with a distance between the rows equal to 15 mm.
- Configuration A3, composed of 3 rows of wooden scatterers of 15 mm diameter, with a distance between rows equal to 15 mm.
- Configuration A4, composed of 4 rows of wooden scatterers of 15 mm diameter, with a distance between rows equal to 15 mm.
- Configuration B1, composed of 1 row of empty scatterers of 20 mm diameter.
- Configuration B2, composed of 2 rows of empty scatterers of 20 mm diameter, with a distance between rows equal to 20 mm.
- Configuration B3, composed of 3 rows of empty scatterers of 20 mm diameter, with a distance between rows equal to 20 mm.
- Configuration B4, composed of 4 rows of empty scatterers of 20 mm diameter, with a distance between rows equal to 20 mm.
- Configuration C1, composed of 1 row of perforated empty scatterers of 20 mm diameter.
- Configuration C2, composed of 1 row of perforated empty scatterers of 20 mm diameter and 1 row of empty scatterers of 20 mm diameter, with a distance between rows equal to 20 mm.

- Configuration C3, composed of 1 row of perforated empty scatterers of 20 mm diameter and 2 rows of empty scatterers of 20 mm diameter, with a distance between rows equal to 20 mm.
- Configuration C4, composed of 1 row of perforated empty scatterers of 20 mm diameter and 3 rows of empty scatterers of 20 mm diameter, with a distance between rows equal to 20 mm.

(type A)

(type B)

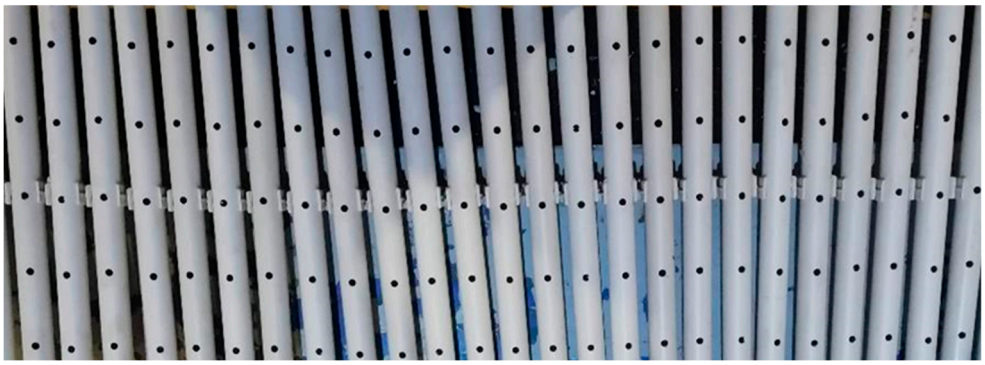

(type C)

**Figure 5.** Wooden scatterers of 15 mm diameter (type A); empty plastic scatterers of 20 mm diameter (type B); empty plastic perforated scatterers of 20 mm diameter.

Figure 6 shows the schemes of all configurations, while Table 1 summarizes the parameters characterizing each configuration.

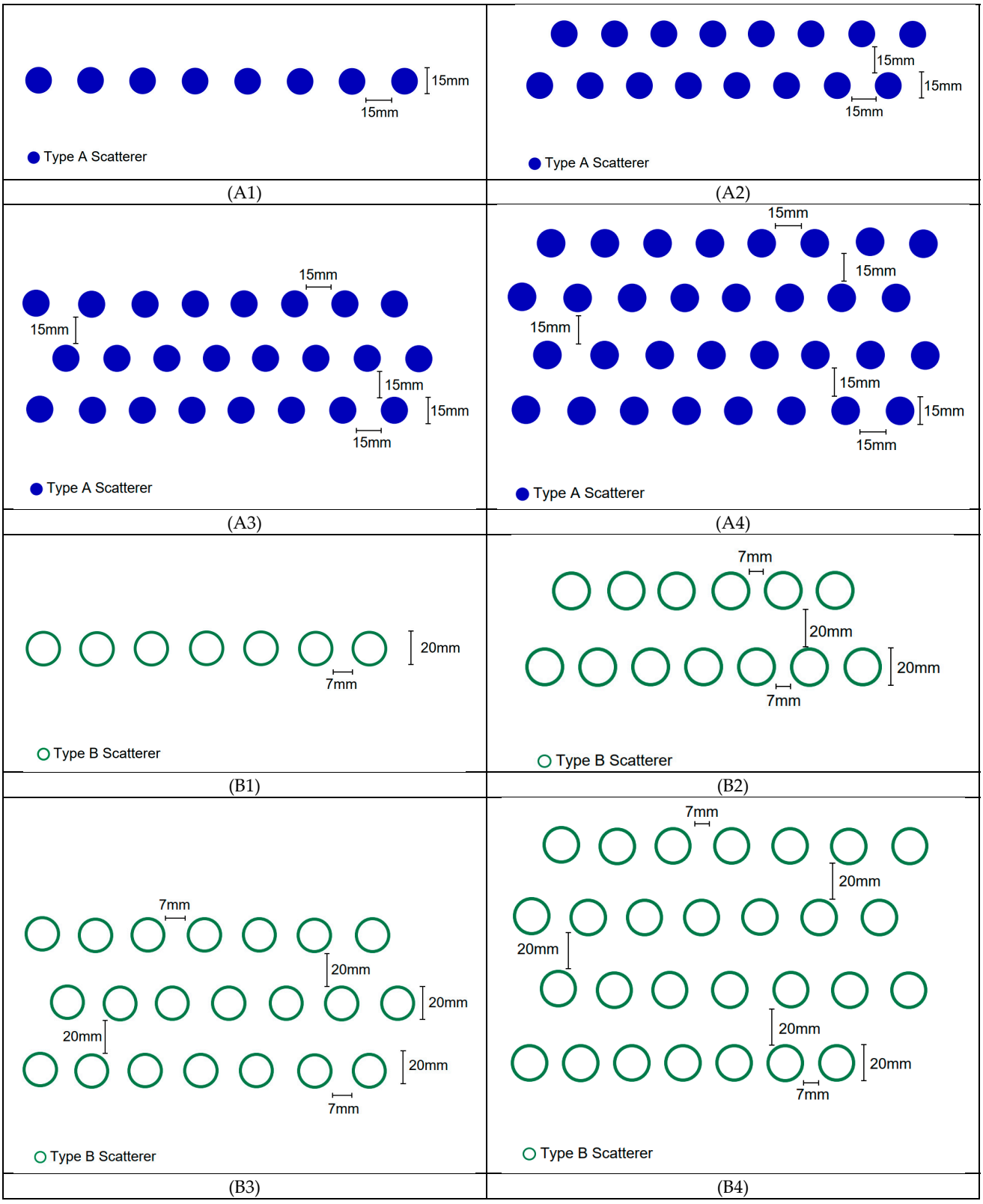
15mm
15mm
Type A Scatterer
(A1)
15mm
15mm
15mm
Type A Scatterer
(A2)
15mm
15mm
15mm
15mm
15mm
Type A Scatterer
(A3)
15mm
15mm
15mm
15mm
15mm
Type A Scatterer
(A4)
20mm
7mm
Type B Scatterer
(B1)
7mm
20mm
20mm
7mm
Type B Scatterer
(B2)
7mm
20mm
20mm
20mm
20mm
7mm
Type B Scatterer
(B3)
7mm
20mm
20mm
20mm
20mm
7mm
Type B Scatterer
(B4)

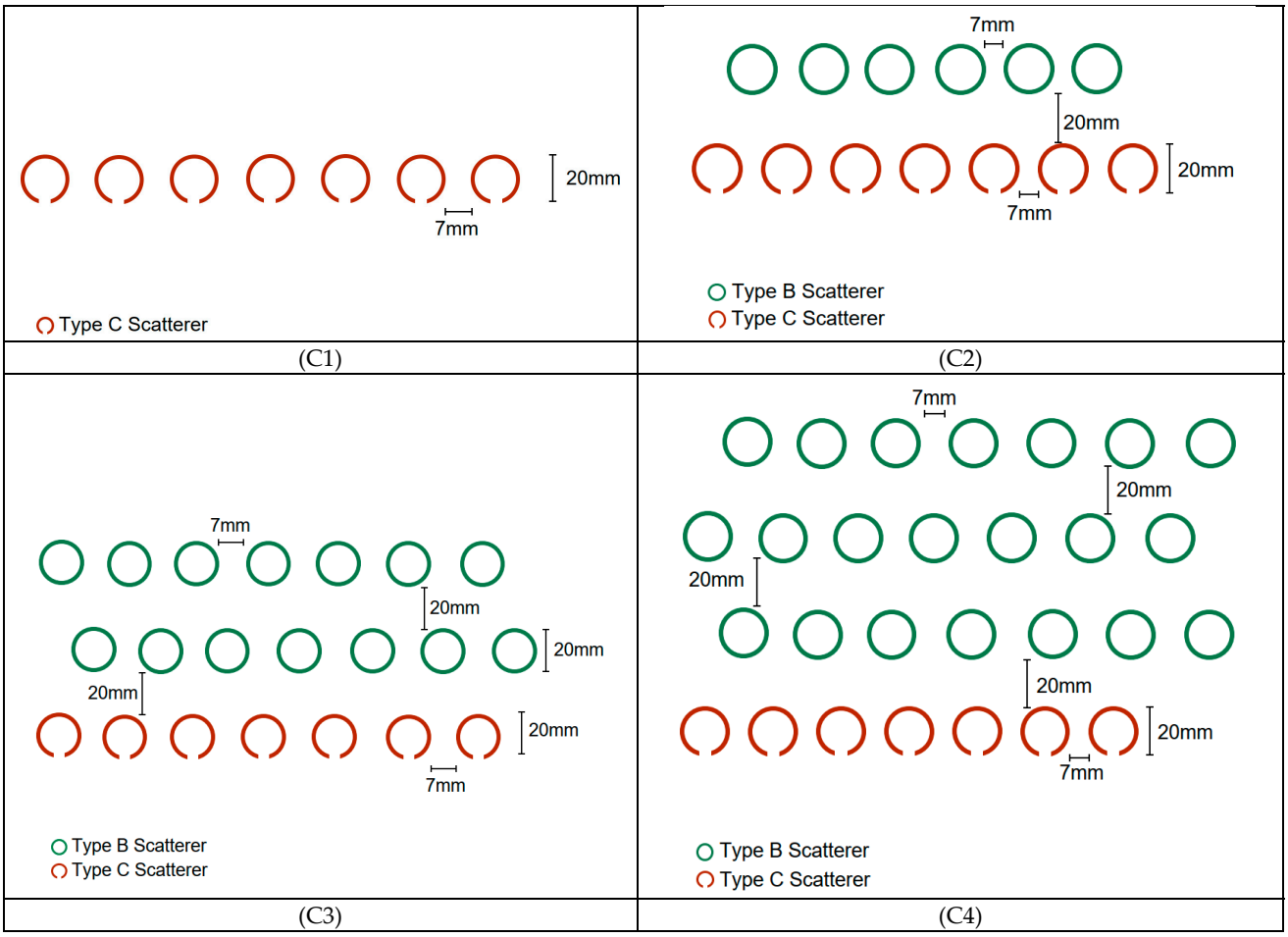


**Figure 6.** Configuration scheme of the test samples.

**Table 1.** Description of all the configurations assumed during the acoustic measurements.

| Configuration | No. of Rows | Distance between Row Layers (mm) | Scatterer Diameter (mm) | Scatterer Distance (mm) |
|---|---|---|---|---|
| A1 | 1 | - | 15 | 15 |
| A2 | 2 | 15 | 15 | 15 |
| A3 | 3 | 15 | 15 | 15 |
| A4 | 4 | 15 | 15 | 15 |
| B1 | 1 | - | 20 | 7 |
| B2 | 2 | 20 | 20 | 7 |
| B3 | 3 | 20 | 20 | 7 |
| B4 | 4 | 20 | 20 | 7 |
| C1 | 1 | - | 20 | 7 |
| C2 | 2 | 20 | 20 | 7 |
| C3 | 3 | 20 | 20 | 7 |
| C4 | 4 | 20 | 20 | 7 |

## 4. Measured Results

The measured *IL* results for all test samples are reported in Figures 7 and 8. Configurations with type A scatterers represent the effect of sound attenuation obtained with plain solid scatterers, where the distance between rows is equal to 15 mm. The scatterers with a cavity, employed in all type B configurations, were analyzed in comparison with

type C configurations, whereas the first row is composed of perforated scatterers (type C) and all the other rows are composed of scatterers with cavity (type B).

The analysis of the results was conducted in the bandwidth between 1 kHz and 10 kHz. The selection of the spectrum analysis is based on the dimensions and size of scatterers; no effects of sound attenuation can be found below 1 kHz because the obstacles/scatterers are seen as acoustically transparent; consistent *IL* results are recorded for octaves above 1 kHz.

Figure 7 shows the *IL* results from type A scatterers. Significant effects of attenuation occur when the system is composed of two or more rows of scatterers, especially at 5 kHz. This peak at 5 kHz increases by incrementing the number of rows, although above this octave band, the attenuation remains constant, approximately around 6 dB. It has been recorded that the attenuation with only one row of scatterers is negligible, giving a maximum *IL* of 3.5 dB only at 5 kHz, while the *IL* is equal to 1 dB on all octaves.

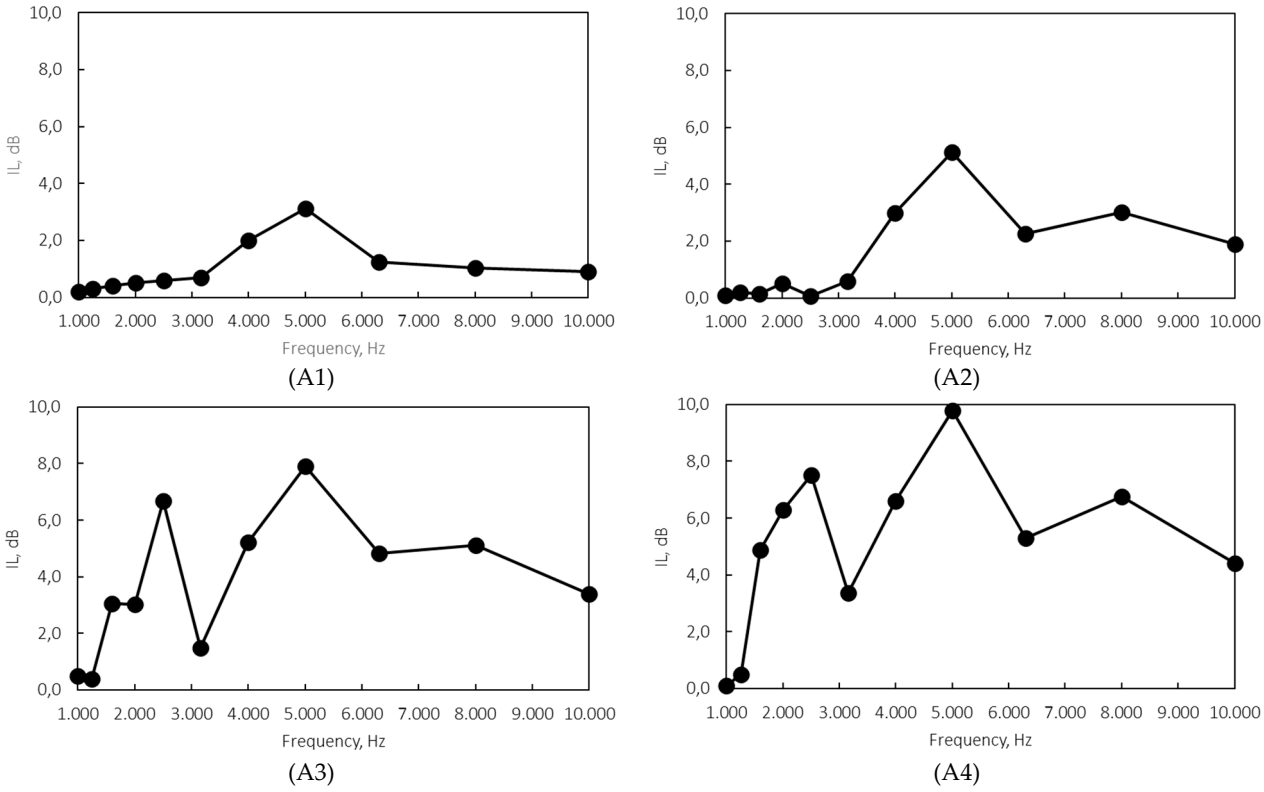


**Figure 7.** Measured results of type A scatterers, composed of 15 mm diameter and a distance of 15 mm between rows of staggered scatterers.

Figure 8 shows the *IL* results from comparisons of the configurations B and C on the same number of rows, where the scatterers are characterized by a 20 mm diameter that can be perforated (type C) or with an enclosed cavity (type B), whereas the distance between scatterers in the same x–y plane is 7 mm. By directly conducting this type of comparison, the effects of perforation on the first row of scatterers are evaluated. The holes are created with the purpose of obtaining a resonant system [35].

With configuration B1, the maximum attenuation is achieved at 5 kHz, equal to 5 dB, while with configuration C1, the maximum attenuation is shifted to 6.3 kHz, equal to 7 dB. A common factor between configurations B1 and C1 occurs across the other octaves, which is very comparable around 1 dB at frequencies below 4 kHz and has the same trendline at 10 kHz.

The same shift in peak is found with configurations B2 and C2, where type B scatterers give an attenuation of 8.5 dB at 5 kHz, while type C gives an attenuation of 10 dB at

6.3 kHz. With the exception of these two peaks, the trendline between configurations B2 and C2 is very comparable.

With three rows of scatterers, the maximum peaks are tuned in the same octaves, recorded at 2.5 kHz and 6.3 kHz, with a very similar trendline. The difference between maximum peaks at the aforementioned octaves is only 1 dB, which is higher with type C scatterers.

With four rows of scatterers, the maximum peaks are found at 2.5 kHz, equal to 7.5 dB with type B and 8.5 dB with type C scatterers, and also at 6.3 kHz, but the difference in attenuation between types B and C scatterers is more accentuated, equal to 11 dB with type B and 8 dB with type C scatterers [36].

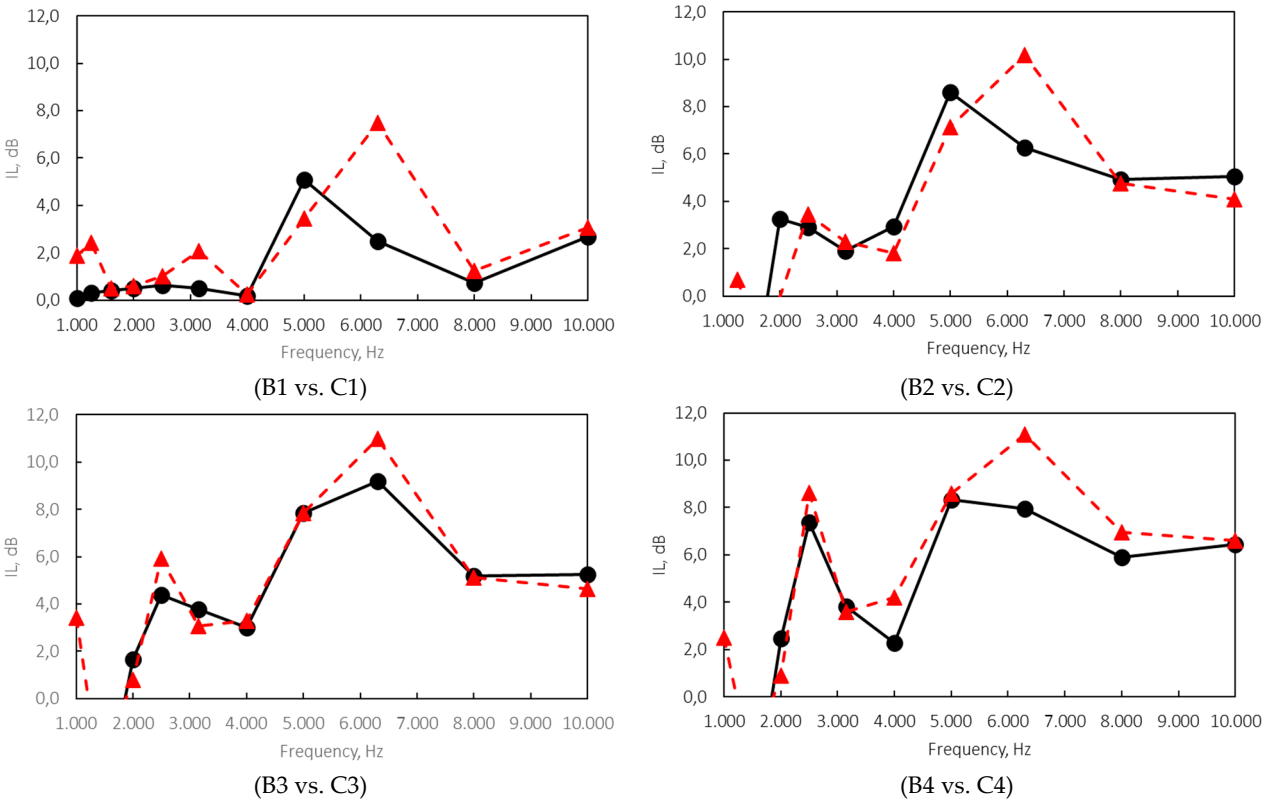


**Figure 8.** Measured results of the comparison of type B and C scatterers with a 20 mm diameter and a distance of 20 mm between rows of staggered scatterers. The continuous black line refers to type B configurations and the dotted red line refers to type C configurations.

## 5. Discussion

The measured results of sound attenuation highlight how similar the acoustic behavior of the scatterers is, although some differences are more visible based on scatterer type and number of rows [37]. Regarding the number of rows, the higher the number, the higher the performance in terms of sound attenuation at high frequencies. Sound attenuation with a single row of type A scatterers is practically negligible. Type A scatterers have significant sound attenuation with three and four rows, reaching an *IL* up to 8 dB at 5 kHz, while the attenuation between 1 kHz and 10 kHz fluctuates around 5 dB. With four rows of type A scatterers, the sound attenuation reaches up to 10 dB at 5 kHz [38].

In terms of type B and C scatterers, the sound attenuation with a single row is recorded at 5 kHz (type B) and 6.3 kHz (type C). By increasing the number of rows, the sound attenuation reaches up to 9 dB at 5 kHz, which is even higher with three rows of scatterers and is very visible with type C scatterers.

Overall, it is recommended that the hybrid system should be tested with more than one type of scatterer, since the performance in terms of sound attenuation is higher [39],

as scientifically tested, when the dimensions and distances are kept the same between scatterers and rows.

## 6. Conclusions

Metamaterial acoustic barriers are widely used for noise attenuation with different applications. One of the many applications includes road traffic noise [40] or HVAC filters. Given the results of this hybrid approach, it can be said that perforated 2D scatterers can be applied to office environments, where the frequencies related to speech are around 1-6 kHz, and are very effective to attenuate female voices [41]. This type of breathable wall/barrier is effective in environments where the solid and opaque partitions are considered to be over designed, especially where the integrity of open spaces must be maintained.

An architectural product that can meet both acoustic and aesthetic requirements may benefit manufacturers in pursuit of a competitive advantage on the market.

Future research studies should focus on more complex geometries of 2D scatterers that can be developed with more sophisticated software, including parametric geometry, which can provide unique sections of scatterers based on the intended attenuation [42]. The following variables play a great role in this process:

- A plenum of cavity bars that can be characterized by helicoidal or other geometric cores [43].
- Different sizes of cavity volumes to better tune the frequencies.
- Holes that can assume different diameters or different shapes (circular, squared, diamond, etc.).

Based on these variables, the idea of creating sound crystals is extensive and requires many test samples [44].

**Author Contributions:** Conceptualization, G.I., G.A., A.B., A.T. and M.C.; methodology, G.I., G.A. and A.T. software, G.I., G.A. and A.T.; validation, G.I., G.A. and A.T.; formal analysis G.I., G.A., A.B., A.T. and M.C.; investigation, G.I., G.A., A.B., A.T. and M.C.; resources, G.I., G.A., A.B., A.T. and M.C.; data curation, G.I., G.A., A.B., A.T. and M.C.; writing—original draft preparation, G.I., G.A., A.B. and M.C.; writing—review and editing, G.I., G.A., A.B. and M.C.; visualization, G.I., G.A., A.B., A.T. and M.C.; supervision G.I., G.A., A.B., A.T. and M.C.; project administration, G.I. and A.T.; funding acquisition, G.I. and A.T. All authors have read and agreed to the published version of the manuscript.

**Funding:** Bio-Acouis (Bio-based Solutions for Improved Acoustic Applications). Received funding through the European Union's project Horizon 2021. Grant agreement No: 101086325.

**Institutional Review Board Statement:** Not applicable.

**Informed Consent Statement:** Not applicable.

**Data Availability Statement:** The original contributions presented in the study are included in the article, further inquiries can be directed to the corresponding author.

**Conflicts of Interest:** The authors declare no conflicts of interest.

## References

1. Pendry, J.B. Negative refraction makes a perfect lens. *Phys. Rev. Lett.* **2000**, *85*, 3966–3969.
2. Munk, B.A. *Metamaterials. Critique and Alternatives*. John Wiley & Sons, Inc.: Hoboken, NJ, USA, 2009.
3. Gupta, A. A Review on Sonic Crystal, Its Applications and Numerical Analysis Techniques. *Acoust. Phys.* **2014**, *60*, 223–234. https://doi.org/10.1134/S1063771014020080.
4. Li, H.; Liu, H.; Zou, J. Minnaert resonances for bubbles in soft elastic materials. *SIAM J. Appl. Math.* **2022**, *82*, 119–141.
5. Iannace, G.; Amadasi, G.; Trematerra, A.; Bevilacqua, A. City-Train noise reduction in urban area by using acoustic mini-screens made of metamaterials. In Proceedings of the Internoise, Tokyo, Japan, 20–23 August 2023.
6. Li, H.; Zou, J. Mathematical theory on dipolar resonances of hard inclusions within a soft elastic material. *arXiv* **2023**, arXiv:2310.12861.
7. Ciaburro, G.; Parente, R.; Iannace, G.; Puyana-Romero, V. Design Optimization of Three-Layered Metamaterial Acoustic Absorbers Based on PVC Reused Membrane and Metal Washers. *Sustainability* **2022**, *14*, 4218. https://doi.org/10.3390/su14074218.

8. Ciaburro, G.; Iannace, G. Membrane-type acoustic metamaterial using cork sheets and attached masses based on reused materials. *Appl. Acoust.* **2022**, *189*, 108605. https://doi.org/10.1016/j.apacoust.2021.108605.
9. Jing, Z.; Xianfeng, W.; Doudou, Z.; Xiaoting, X.; Xiaoting, W.; Xiaopeng, Z. Amber rainbow ribbon effect in broadband optical metamaterials. *Nat. Commun.* **2024**, *15*, 2613.
10. Sgarlato, N.; Sgarlato, A. *Secret Projects of the Kriegsmarine: Unseen Designs of Nazi Germany's Navy*; Greenhill Books: Barnsley, UK, 2022. ISBN 978-1-78438-687-0. OCLC 1260821096.
11. Sharma, G.S.; Skvortsov, A.; MacGillivray, I.; Kessissoglou, N. Sound absorption by rubber coatings with periodic voids and hard inclusions. *Appl. Acoust.* 2019, 143, pp. 200–210.
12. Méresse, P.; Audoly, C.; Croënne, C.; Hladky-Hennion, A.C. Acoustic coatings for maritime systems applications using resonant phenomena. *Comptes Rendus Mécanique* **2015**, *343*, 645–655.
13. Audoly, C. Perspectives of Metamaterials for Acoustic Performances of Submerged Platforms and Systems. In Proceedings of the Undersea Defence Technology Conference 2016, Oslo, Norway, 1–3 June 2016.
14. Ziolkowski, R.W. Metamaterials: the early years in the USA. *EPJ Appl. Metamate.* **2014**, *1*, 1–9.
15. Walser, R.M. *Complex Mediums II: Beyond Linear Isotropic Dielectrics*; Lakhtakia, A., Ed.; SPIE: Bellingham, WA, USA, 2001.
16. Veselago, V.G. The electrodynamics of substance with simultaneously negative values of ε and μ. *Sov. Phys. Usp.* **1968**, *10*, 509–524.
17. Boardman, A. Pioneers in metamaterials: John Pendry and Victor Veselago. *J. Opt.* **2011**, *13*, 2. https://doi.org/10.1088/2040-8978/13/2/020401.
18. Pendry, J.B.; Li, J. An acoustic metafluid: realizing a broadband acoustic cloak. *New J. Phys.* **2008**, *10*, 115032.
19. Sánchez-Pérez, J.V.; Caballero, D.; Rubio, C.; Martínez-Sala, R.; Sánchez Dehesa, J.; Meseguer, F.; Llinares, J.; Gálves, F. Sound attenuation by a two dimensional arrays of rigid cylinders. *Phys. Rev. Lett.* **1998**, *80*, 5325–5328.
20. Martinez-Sala, R.; Sancho, J.; Sanchez, J.V.; Gomez, V.; Llinarez, J.; Meseguer, F. Sound attenuation by sculpture. *Nature* **1995**, *378*, 241.
21. Lincoln, R.L.; Scarpa, F.; Ting, V.P.; Trask, R.S. Multifunctional composites: a metamaterial perspective. *Multifunct. Mater.* **2019**, *2*, 043001.
22. Iannace, G.; Berardi, U.; Ciaburro, G.; Trematerra, A. Sound attenuation of an acoustic barrier made with metamaterials. *Can. Acoust.-Acoust. Can.* **2019**, *47*, 5–9.
23. Bevilacqua, A.; Iannace, G.; Lombardi, I.; Trematerra, A. 2D Sonic Acoustic Barrier Composed of Multiple-Row Cylindrical Scatterers: Analysis with 1:10 Scaled Wooden Models. *Appl. Sci.* **2022**, *12*, 6302. https://doi.org/10.3390/app12136302
24. Donnelly, D.; La Spada, L. Electromagnetic and thermal nanostructures: from waves to circuits. *Eng. Res. Express* **2020**, *2*, 015045. https://doi.org/10.1088/2631-8695/ab7a78.
25. Iannace, G.; Ciaburro, G.; Trematerra, A. Heating, ventilation, and air conditioning (HVAC) noise detection in open-plan offices using recursive partitioning. *Buildings* **2018**, *8*, 169. https://doi.org/10.3390/buildings8120169
26. Piana, E.A.; Carlsson, U.E.; Lezzi, A.M.; Paderno, D.; Boij, S. Silencer Design for the Control of Low Frequency Noise in Ventilation Ducts. *Designs* **2022**, *6*, 37. https://doi.org/10.3390/designs6020037
27. Liu, Z.; Zhang, X.; Mao, Y.; Zhu, Y.Y.; Yang, Z.; Chan, C.T.; Sheng, P. Locally resonant sonic materials. *Science* **2000**, *289*, 1734–1736.
28. Sabat, R.; Cochin, E.; Kalderon, M.; Lévêque, G.; Antoniadis, I.; Djafari-Rouhani, B.; Pennec, Y. Low frequency sound isolation by a metasurface of Helmholtz ping-pong ball resonators featured. *J. Appl. Phys.* **2023**, *134*, 144502. https://doi.org/10.1063/5.0160267
29. Torrent, D.; Sánchez-Dehesa, J. Anisotropic mass density by two-dimensional acoustic metamaterials. *New J. Phys.* **2008**, *10*, 023004.
30. Cummer ,S.A.; Schurig, D. One path to acoustic cloaking. *New J. Phys.* **2007**, *9*, 45.
31. Pai, P.F.; Huang, G. *Theory and Design of Acoustic Metamaterials*; SPIE: Bellingham, WA, USA, 2015.
32. Ciaburro, G.; Iannace, G. Numerical Simulation for the Sound Absorption Properties of Ceramic Resonators. *Fibers* **2020**, *8*, 77. https://doi.org/10.3390/fib8120077.
33. CLIO System. Available online: http://www.audiomatica.com/ (accessed on 16 May 2024).
34. Craster, R.V.; Guenneau, S. *Acoustic Metamaterials: Negative Refraction, Imaging, Lensing and Cloaking*. Springer: Berlin/Heidelberg, Germany, 2013.
35. Lagarrigue, C.; Groby, J.P.; Tournat, V. Sustainable sonic crystal made of resonating bamboo rods. *J. Acoust. Soc. Am.* **2013**, *133*, 247–254. https://doi.org/10.1121/1.4769783.
36. Elayouch, A.; Addouche. M.; Khelif, A.; Wide tailorability of sound absorption using acoustic metamaterials. *Appl. Phys.* **2017**, *124*, 155103. https://doi.org/10.1063/1.5035129.
37. Ciaburro, G.; Iannace, G.; Trematerra, A. Sound attenuation with metamaterials. In Proceedings of the 19th Conference on Applied Mathematics, APLIMAT 2020 Proceedings 2020, Bratislava, Slovakia, 4–6 February 2020; pp. 283–292.
38. Iannace, G.; Ciaburro, G.; Trematerra, A. Metamaterials acoustic barrier. *Appl. Acoust.* **2021**, *181*, 108172. https://doi.org/10.1016/j.apacoust.2021.108172.
39. Naify, C.J.; Chang, C.M.; McKnight, G.; Nutt, S.R. Scaling of membrane-type locally resonant acoustic metamaterial arrays. *J. Acoust. Soc. Am.* **2012**, *132*, 2784–2792. https://doi.org/10.1121/1.4744941.
40. Tronchin, L. On the acoustic efficiency of road barriers: The reflection index. *Int. J. Mech.* **2013**, *7*, 318–326.

41. Ghaffarivardavagh, R.; Nikolajczyk, J.; Anderson, S.; Zhang, X. Ultra-open acoustic metamaterial silencer based on Fano-like interference. *Phys. Rev. B* **2019**, *99*, 024302. https://doi.org/10.1103/PhysRevB.99.024302.
42. Ciaburro, G.; Iannace, G. Modeling acoustic metamaterials based on reused buttons using data fitting with neural network. *J. Acoust. Soc. Am.* **2021**, *150*, 51–63. https://doi.org/10.1121/10.0005479.
43. Pozar, D.M. Microwave engineering education: from field theory to circuit theory. In Proceedings of the 2012 IEEE/MTT-S International Microwave Symposium Digest, Montreal, QC, Canada, 17–22 June 2012.
44. Czwielong, F.; Hruška, V.; Bednařík, M.; Becker, S. On the acoustic effects of sonic crystals in heat exchanger arrangements. *Appl. Acoust.* **2021**, *182*, 108253.